Localized Partial Oxidation of Acetic Acid at the Dual Perimeter Sites of the Au/TiO$_2$ Catalyst—Formation of Gold Ketenylidene

Isabel Xiaoye Green,[†] Wenjie Tang,[‡] Matthew Neurock,[†,‡] and John T. Yates, Jr.*[,†,‡]

Departments of [†]Chemistry and [‡]Chemical Engineering, University of Virginia, Charlottesville, Virginia 22904, United States

S *Supporting Information*

ABSTRACT: Chemisorbed acetate species derived from the adsorption of acetic acid have been oxidized on a nano-Au/TiO$_2$ (~3 nm diameter Au) catalyst at 400 K in the presence of O$_2$(g). It was found that partial oxidation occurs to produce gold ketenylidene species, Au$_2$=C=C=O. The reactive acetate intermediates are bound at the TiO$_2$ perimeter sites of the supported Au/TiO$_2$ catalyst. The ketenylidene species is identified by its measured characteristic stretching frequency ν(CO) = 2040 cm^{-1} and by ^{13}C and ^{18}O isotopic substitution comparing to calculated frequencies found from density functional theory. The involvement of dual catalytic Ti^{4+} and Au perimeter sites is postulated on the basis of the absence of reaction on a similar nano-Au/SiO$_2$ catalyst. This observation excludes low coordination number Au sites as being active alone in the reaction. Upon raising the temperature to 473 K, the production of CO$_2$ and H$_2$O is observed as both acetate and ketenylidene species are further oxidized by O$_2$(g). The results show that partial oxidation of adsorbed acetate to adsorbed ketenylidyne can be cleanly carried out over Au/TiO$_2$ catalysts by control of temperature.

The scarcity of fossil fuels along with the increasing price of oil has stimulated significant efforts in the utilization of other forms of renewable energy such as biomass. Acetic acid, which is one of the most common products in the conversion of biomass, has gained considerable attention.[1] The transformation of acetic acid into other useful products is currently one of the key issues in the development of optimal economic strategies for the conversion of biomass. Novel Au oxidation catalysts which have demonstrated remarkable catalytic performance for the selective oxidation of CO and other hydrocarbon sources[2−4] also show promising potential for oxidation processes that convert acetic acid to valuable unsaturated hydrocarbon intermediates via the selective removal of hydrogen.

Experiment as well as theory have shown that dual perimeter sites for nanometer Au/TiO$_2$ catalysts which involve both Au and Ti^{4+} centers, located at the interface of the Au nanoparticles and the TiO$_2$ support, catalyze oxidation reactions by dissociating O$_2$ molecules at these sites.[5−8] In this paper, we show that these localized Au−Ti perimeter sites can catalytically oxidize acetic acid to a novel gold ketenylidene surface intermediate (Au$_2$=C=C=O, also known as gold ketenide). This species is produced by the activation of the C−H bonds in the methyl group of chemisorbed CH$_3$COO/TiO$_2$ at the Au/TiO$_2$ perimeter, subsequently following the breaking of one C=O bond.

The study of ketenylidene species (CCO) has taken place over a century since the first synthesis of ketene in 1905.[9] It is considered an important intermediate in hydrocarbon combustion,[10−13] in Fischer−Tropsch catalysis,[14−18] (but see ref 19), and even in present-day astrochemistry.[20] Most metal ketenylidene species are synthesized as complexes with CCO ligands centered on transition metal atoms, such as Ru,[14] Fe,[21] Os,[21] Ta,[15] Zr,[22] Hf,[17] or Pt,[23] or are observed during Cu thin-film growth using a Cu organometallic complex.[24] A set of group 11 metal (Cu, Ag, Au) ketenylidenes was synthesized from corresponding salts.[25−27] The detection of ketenylidene species by spectroscopic measurements is typically confirmed by theoretical simulations.[23,28−30] Since the proposal of possible surface ketenylidene species by Shriver et al. in 1987,[14] only two documented cases of ketenylidene detection were reported on well-characterized surfaces: acetone was reacted with a preoxidized Ag(111) surface,[16,31] and CO was deposited on a W$_2$C(0001) surface.[32] Herein, we show for the first time the spectroscopic observation of gold ketenylidene formation on a TiO$_2$-supported Au catalyst from the partial oxidation of acetic acid at Au−Ti dual perimeter sites at the interface using O$_2$(g). The reaction is particularly interesting mechanistically because the acetic acid reactant dissociatively adsorbs to form a carboxylate (CH$_3$COO$^-$) intermediate on the TiO$_2$ support while the product, ketenylidene, is bound to the gold nanoparticles as a Au$_2$=C=C=O species.

The Au/TiO$_2$ catalyst (with Au particles possessing a mean diameter of ~3 nm, Supporting Information, Figure S1) was synthesized using the deposition−precipitation protocol from HAuCl$_4$, TiO$_2$ powder (Degussa P25), and urea as developed by Zanella et al.[33] Following synthesis, the Au/TiO$_2$ catalyst and a blank TiO$_2$ sample were pressed separately as 7 mm diameter spots into a tungsten grid and mounted into a high-vacuum transmission IR cell that was described in detail previously.[7,8] To activate and regenerate the catalyst before each experiment, a standard annealing treatment at 473 K was carried out. The treatment includes heating in vacuum for 30 min and oxidation by 18 Torr of O$_2$ for 210 min, followed by evacuation for 10 min. This annealing procedure removes most of the hydrocarbon species accumulated on the catalyst during its preparation, as observed by IR spectroscopy. Annealing at higher temperature was avoided to minimize possible sintering

of Au particles during treatment. The samples were cooled to reaction temperatures between 370 and 400 K as described in each experiment after the annealing treatment.

Figure 1 shows the IR spectra of saturated adsorbed acetate (from acetic acid) on the Au/TiO_2 catalyst and on the TiO_2
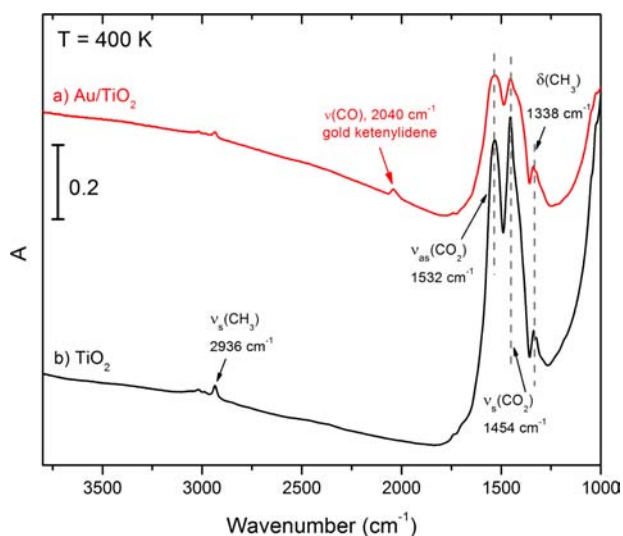

Figure 1. IR spectra of acetate species (from acetic acid) adsorbed on (a) Au/TiO_2 and (b) TiO_2 at 400 K.

blank sample at 400 K after evacuation of gas-phase acetic acid. The four main features observed at 2936 cm^{-1} (symmetric CH_3 stretching), 1532 cm^{-1} (asymmetric CO_2 stretching), 1454 cm^{-1} (symmetric CO_2 stretching), and 1338 cm^{-1} (CH_3 deformation) match well with other reported acetate ion adsorption features on TiO_2.[34] The resemblance between the two spectra indicates that acetic acid dissociatively adsorbs on the TiO_2 surface to produce acetate. A weak feature at 2040 cm^{-1} is uniquely observed on the Au/TiO_2 sample and is attributed to the acetate partial oxidation product—gold ketenylidene.[35] We postulate that this new species comes from acetate reacting with the adsorbed oxygen left over from the annealing treatment of the Au/TiO_2 catalyst. The unique 2040 cm^{-1} band corresponds to the C=O stretching motion and falls into the observed frequency range of 2004−2076 cm^{-1} for other reported ketenylidene ligands[14,15,17,24,35] and the silver ketenylidene surface species.[31] The other reported vibrational frequencies of gold ketenylidene species (ν_{Au-C} at 428 cm^{-1}; δ_{CCO} at 562 cm^{-1})[35] are below the natural spectral cutoff of TiO_2 ($\sim$1000 cm^{-1}), and thus are not observed.

When the adsorbed acetate on the Au/TiO_2 catalyst as reported in Figure 1a comes into contact with 1 Torr of gas-phase O_2 at 400 K, the band at 2040 cm^{-1} increases immediately in absorbance as shown in Figure 2, indicating an increase in coverage of the surface ketenylidene species due to CH_3COO/TiO_2 oxidation. Gold ketenylidene appears to be the first and only oxidation product observed by IR from adsorbed acetate ion at 400 K. No gas-phase CO_2 was detected during the 90 min experiment, indicating a lack of total oxidation at 400 K on the Au/TiO_2 catalyst. However, during the annealing treatment in O_2 at 473 K carried out to restore the catalyst surface, all adsorbed acetate and ketenylidene species were oxidized to CO_2 and H_2O, judging from the IR spectra (not shown). This behavior gives evidence for temperature-controlled oxidation. No reaction was detected
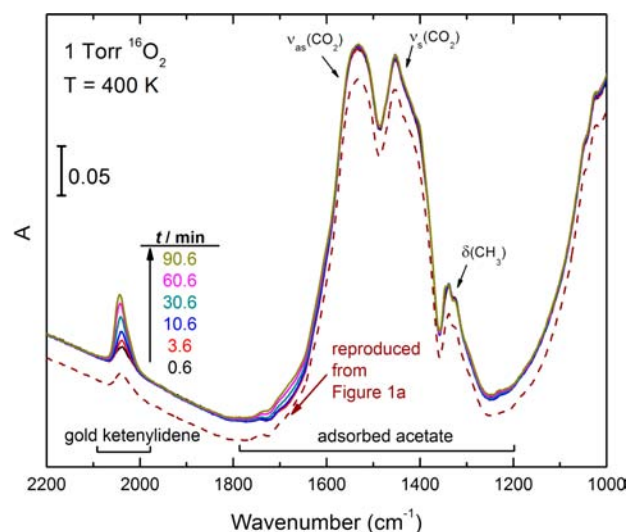

Figure 2. IR spectra (solid lines) of the acetate partial oxidation process on the Au/TiO_2 catalyst at 400 K under 1 Torr of O_2(g). Dotted spectrum: before O_2 exposure (reproduced spectrum from Figure 1a).

from the IR observations on the TiO_2 blank sample under the same experimental conditions for 90 min, indicating that gold is necessary for the catalytic oxidation of acetate.

To further confirm the role of the Au−Ti dual perimeter sites, a Au/SiO_2 sample with a similar average gold particle size ($\sim$2.5 nm) was synthesized by Zanella et al.[36] and tested in our laboratory. Pretreatment and experimental conditions identical to those employed for the Au/TiO_2 sample were used on the Au/SiO_2 sample, but no ketenylidene species were detected at 400 K under 1 Torr of O_2(g), as shown in Figure 3c. The adsorbed acetate in the SiO_2 spectrum matches with literature reports, where acetic acid deprotonates on the SiO_2 surface.[37] Hydrogen bonding between the carbonyl group and the highly
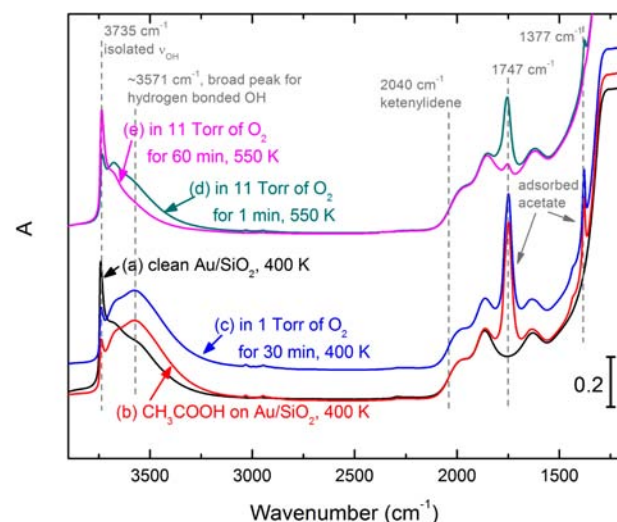

Figure 3. IR spectra of an acetic acid oxidation experiment similar to that depicted in Figure 2 but on a Au/SiO_2 sample. Spectra a−e are taken in one experiment sequentially: (a) clean hydroxylated Au/SiO_2 sample at 400 K; (b) adsorbed acetic acid on Au/SiO_2 at 400 K; (c) after contact with 1 Torr of O_2 at 400 K for 30 min; (d) ramp up temperature to 550 K and increase O_2 pressure to 11 Torr for 1 min; (e) 11 Torr of O_2 at 550 K for 60 min.

hydroxylated SiO₂ surface also occurs, indicated by the intensity decrease of the isolated Si−OH band at 3735 cm⁻¹ and the increase of the broad band ~3571 cm⁻¹ for hydrogen-bonded Si−OH groups.[37] The obvious differences between the acetate/Au/SiO₂ spectrum (Figure 3b) and the acetate/Au/TiO₂ spectrum (Figure 1) again confirm that the acetate observed in Figure 1 is adsorbed on TiO₂ and not on Au.

To be sure that the Au/SiO₂ sample is inactive toward acetic acid oxidation, the reaction temperature was increased to 550 K with an increased oxygen pressure of 11 Torr. Under these conditions, the loss of adsorbed acetate/SiO₂ species was observed during the 60 min experiment shown in Figure 3d,e, but no gold ketenylidene species were detected by IR spectroscopy. The negative result from the Au/SiO₂ sample shown in Figure 3 compared to the observed catalytic activity on the Au/TiO₂ catalytic sites for oxidation of CH₃COO/TiO₂ indicates that the oxidation requires both a Ti site and a Au site, and that low-coordinate Au sites present on Au/SiO₂ are insufficient for ketenylidene formation.

In a separate set of experiments, we found that acetate and gold ketenylidene are also the final products of ethylene partial oxidation on a Au/TiO₂ catalyst at 370 K. Utilizing this property, we used isotope-labeled ¹³C₂H₄ to confirm the vibrational assignment of gold ketenylidene. Figure 4 shows the
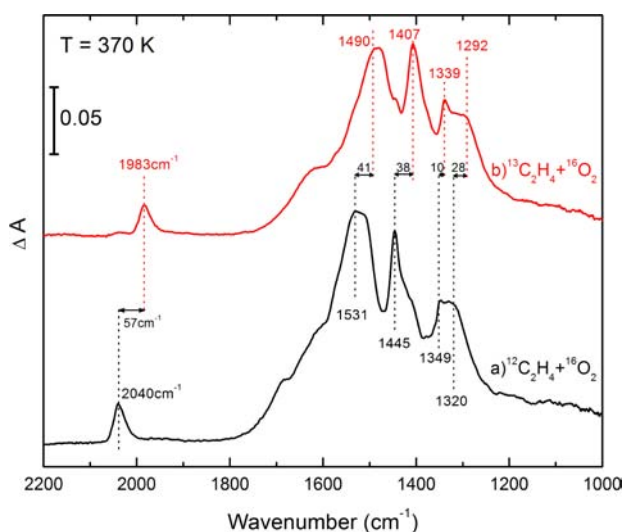

Figure 4. ¹³C-isotopic study of gold ketenylidene formation from ethylene oxidation on Au/TiO₂ catalyst. Spectra taken after 90 min of reaction at 370 K with 0.5 Torr of ethylene and 0.5 Torr of O₂. (a) ¹²C₂H₄ study. (b) ¹³C₂H₄ study.
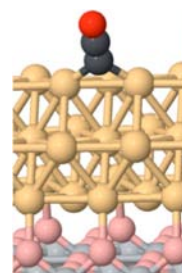
oxidation products of a mixture of 0.5 Torr ¹²C₂H₄ and 0.5 Torr O₂, compared with the oxidation products of a mixture of 0.5 Torr ¹³C₂H₄ and 0.5 Torr O₂, on the Au/TiO₂ catalyst at 370 K. Acetate and gold ketenylidene features are observed during the reaction as shown in Figure 4. The ¹³C substitution caused a red shift for every vibrational feature observed in acetate and gold ketenylidene. A 57 cm⁻¹ red shift was measured for Au₂=¹³C=¹³C=¹⁶O (1983 cm⁻¹) compared to Au₂=¹²C=¹²C=¹⁶O (2040 cm⁻¹). In addition to ¹³C isotope labeling, we also used ¹⁸O (99%) to oxidize ethylene. A Au₂=¹²C=¹²C=¹⁸O adsorption band at 2010 cm⁻¹ was observed (spectrum not shown), red-shifted 30 cm⁻¹ from the non-labeled Au₂=¹²C=¹²C=¹⁶O species.

To rationalize these frequency shifts, we carried out first-principles density functional theory (DFT) calculations to

simulate the chemisorbed gold ketenylidene structure and its corresponding frequencies. We used a (2×3) unit cell to simulate the surface rutile TiO₂(110) structure, with four O−Ti−O trilayers stacked in the Z-direction. The 3 nm Au particle on TiO₂ is simulated by a close-packed Au nanorod that has 3-Au atomic-layer height and infinite length. This model provides a reliable description of the Au surface with different Au atom coordination number (CN) sites and was used previously by other groups and ourselves to model catalytic reactions at the Au/TiO₂ interfaces.[5,7,8,38] More details of the model structure and calculation can be found in the Supporting Information.

We surveyed the entire Au/TiO₂ model surface and calculated the most probable adsorption sites in order to find the most stable configurations for the ketenylidene species, including the Au and Ti₅c sites at the Au/TiO₂ perimeter, as well as the Ti₅c sites removed from the interface. The linear ketenylidene species preferentially binds to the bridge Au−Au edge site (CN=7) at the top of the Au cluster to form a Au₂=C=C=O species that is oriented away from the edge, as shown in Table 1. The adsorption energy of ketenylidene at

Table 1. Comparison of Experimentally Measured Gold Ketenylidene Isotopically Labeled Species Frequencies and DFT-Calculated Frequencies

	Species	v(DFT) (cm⁻¹)	v(Exp) (cm⁻¹)
	Au₂=¹²C=¹²C=¹⁶O	2041	2040
	Au₂=¹³C=¹³C=¹⁶O	1980	1983
	Au₂=¹²C=¹²C=¹⁸O	2016	2010

this site was calculated to be −3.85 eV (Figure S2a), which is significantly larger than those for the other configurations examined, including the formation of a di-σ-bound Ti₅c−C=C=O−Ti₅c intermediate which lies parallel to the TiO₂ surface (−2.77 eV, Figure S2b) and the formation of (Ti₅c)₂=C=C=O intermediates oriented normal to the TiO₂ support removed from the Au nanorod (−2.52 eV, Figure S2c) as well as at interfacial Ti₅c−Ti₅c sites at the Au perimeter (−2.32 eV, Figure S2d).

In addition to Au₂ being the most stable adsorption site for ketenylidene, it also results in the closest theoretical ν(C=O) vibrational frequency (2041 cm⁻¹) to the band frequency measured experimentally (2040 cm⁻¹) for the non-isotope-labeled gold ketenylidene species. The calculated vibrational frequencies for ketenylidene adsorbed on the various Ti₅c sites (Figure S2) differ from the experimental measured value by more than 30 cm⁻¹. Comparisons of the calculated isotopic shift of the ν(C=O) frequency for the Au₂=C=C=O configuration to the experimental measurements are summarized in Table 1. The almost exact match of absolute frequencies shown in Table 1 is a happy coincidence from DFT simulation. The direction and magnitude of frequency shifts from calculated isotope substitution matches the experimental measurements, confirming the observation of the production of gold ketenylidene chemisorbed species from the partial oxidation of CH₃COO/TiO₂.

The catalytic partial oxidation of acetate ion adsorbed on TiO₂ to form gold ketenylidene at the dual perimeter sites of

the Au/TiO$_2$ catalyst thus appears to proceed through a series of steps involving C−H bond scission and C−O bond scission. We postulate that the C−H bond scission is activated by the atomic O generated from O$_2$(g) dissociation at the Au−Ti dual perimeter sites.[7,8] Following C−H bond scission, the Au−C bonds start to form, which facilitates the activation of the C−O bond at the Ti cationic sites. A schematic of the oxidation process from CH$_3$COO/TiO$_2$ to the O=C=C/Au intermediate is shown in Figure 5.
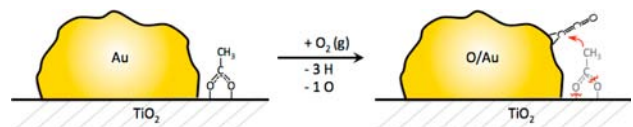

Figure 5. Scheme of the catalytic oxidation of CH$_3$COO/TiO$_2$ at the perimeter of the Au/TiO$_2$ particle, forming Au$_2$=C=C=O.

To the best of our knowledge, this is the first report of the catalytic oxidation of acetate (and ethylene) to ketenylidene over a supported Au catalyst. The gold ketenylidene species formed at temperatures around 400 K can be further oxidized to CO$_2$ and H$_2$O at 473 K on the same catalyst, illustrating that the depth of the catalytic oxidation can be controlled by varying the reaction temperature. The acetate-to-ketenylidene formation path is a combination of dehydrogenation (oxidation) and deoxygenation of chemisorbed acetate, which are crucial steps for biomass conversion into more valuable industrial chemicals.

■ ASSOCIATED CONTENT

Ⓢ Supporting Information
Detailed description of the calculation parameters as well as extra calculation results. This material is available free of charge via the Internet at http://pubs.acs.org.

■ AUTHOR INFORMATION

Corresponding Author
johnt@virginia.edu
Notes
The authors declare no competing financial interest.

■ ACKNOWLEDGMENTS

■ REFERENCES

(1) Munasinghe, P. C.; Khanal, S. K. *Bioresour. Technol.* **2010**, *101*, 5013.
(2) Haruta, M.; Kobayashi, T.; Sano, H.; Yamada, N. *Chem. Lett.* **1987**, *2*, 405.
(3) Meyer, R.; Lemire, C.; Shaikhutdinov, S. K.; Freund, H.-J. *Gold Bull.* **2004**, *37*, 72.
(4) Haruta, M. *CATTECH* **2002**, *6*, 102.
(5) Laursen, S.; Linic, S. *Phys. Chem. Chem. Phys.* **2009**, *11*, 11006.
(6) Wang, J. G.; Hammer, B. *Phys. Rev. Lett.* **2006**, *97*, 136107.
(7) Green, I. X.; Tang, W.; Neurock, M.; Yates, J. T., Jr. *Science* **2011**, *333*, 736.
(8) Green, I. X.; Tang, W.; Neurock, M.; Yates, J. T., Jr. *Angew. Chem., Int. Ed.* **2011**, *50*, 10186.
(9) Staudinger, H. *Ber. Dtsch. Chem. Ges.* **1905**, *38*, 1735.
(10) Bayes, K. D. *J. Chem. Phys.* **1970**, *52*, 1093.
(11) Fontijn, A.; Johnson, S. E. *J. Chem. Phys.* **1973**, *59*, 6193.
(12) Sault, A. G.; Madix, R. J. *J. Phys. Chem.* **1986**, *90*, 4723.
(13) Sault, A. G.; Madix, R. J. *Surf. Sci.* **1986**, *172*, 598.
(14) Sailor, M. J.; Shriver, D. F. *J. Am. Chem. Soc.* **1987**, *109*, 5039.
(15) Neithamer, D. R.; LaPointe, R. E.; Wheeler, R. A.; Richeson, D. S.; Van Duyne, G. D.; Wolczanski, P. T. *J. Am. Chem. Soc.* **1989**, *111*, 9056.
(16) Sim, W. S.; King, D. A. *J. Am. Chem. Soc.* **1995**, *117*, 10583.
(17) Calderazzo, F.; Englert, U.; Guarini, A.; Marchetti, F.; Pampaloni, G.; Segre, A.; Tripepi, G. *Chem.—Eur. J.* **1996**, *2*, 412.
(18) Deng, L.-J.; Huo, C.-F.; Liu, X.-W.; Zhao, X.-H.; Li, Y.-W.; Wang, J.; Jiao, H. *J. Phys. Chem. C* **2010**, *114*, 21585.
(19) Blyholder, G.; Emmett, P. H. *J. Phys. Chem.* **1960**, *64*, 470.
(20) Ohishi, M.; Suzuki, H.; Ishikawa, S. I.; Yamada, C.; Kanamori, H.; Irvine, W. M.; Brown, R. D.; Godfrey, P. D.; Kaifu, N. *Astrophys. J.* **1991**, *380*, L39.
(21) Shriver, D. F.; Sailor, M. J. *Acc. Chem. Res.* **1988**, *21*, 374.
(22) Calderazzo, F.; Englert, U.; Guarini, A.; Marchetti, F.; Pampaloni, G.; Segre, A. *Angew. Chem., Int. Ed. Engl.* **1994**, *33*, 1188.
(23) Bertani, R.; Casarin, M.; Ganis, P.; Maccato, C.; Pandolfo, L.; Venzo, A.; Vittadini, A.; Zanotto, L. *Organometallics* **2000**, *19*, 1373.
(24) Girolami, G. S.; Jeffries, P. M.; Dubois, L. H. *J. Am. Chem. Soc.* **1993**, *115*, 1015.
(25) Blues, E. T.; Bryce-Smith, D.; Hirsch, H.; Simons, M. J. *J. Chem. Soc. D: Chem. Commun.* **1970**, XXX.
(26) Blues, E. T.; Bryce-Smith, D.; Kettlewell, B.; Roy, M. *J. Chem. Soc., Chem. Commun.* **1973**, XXX.
(27) Blues, E. T.; Bryce-Smith, D.; Lawston, I. W.; Wall, G. D. *J. Chem. Soc., Chem. Commun.* **1974**, 513.
(28) Sailor, M. J.; Went, M. J.; Shriver, D. F. *Inorg. Chem.* **1988**, *27*, 2666.
(29) Li, J.; Bursten, B. E.; Zhou, M.; Andrews, L. *Inorg. Chem.* **2001**, *40*, 5448.
(30) Casarin, M.; Pandolfo, L. *J. Organomet. Chem.* **2003**, *682*, 255.
(31) Sim, W. S.; King, D. A. *J. Phys. Chem.* **1996**, *100*, 14794.
(32) Aizawa, T.; Otani, S. *J. Chem. Phys.* **2011**, *135*, 144704.
(33) Zanella, R.; Giorgio, S.; Henry, C. R.; Louis, C. *J. Phys. Chem. B* **2002**, *106*, 7634.
(34) Liao, L.-F.; Lien, C.-F.; Lin, J.-L. *Phys. Chem. Chem. Phys.* **2001**, *3*, 3831.
(35) Blues, E.; Bryce-Smith, D.; Lawston, I. *Gold Bull.* **1976**, *9*, 88.
(36) Zanella, R.; Sandoval, A.; Santiago, P.; Basiuk, V. A.; Saniger, J. M. *J. Phys. Chem. B* **2006**, *110*, 8559.
(37) Young, R. P. *Can. J. Chem.* **1969**, *47*, 2237.
(38) Molina, L. M.; Rasmussen, M. D.; Hammer, B. *J. Chem. Phys.* **2004**, *120*, 7673.